Contribution from the Baker Laboratory of Chemistry,
Cornell University, Ithaca, New York 14853

Superconductivity, Magnetic Susceptibility, and Magnetic Resonance Studies of the Pseudobinary Systems $Eu_{1.2}Mo_6S_8$-$Eu_{1.2}Mo_6Se_8$ and $LaMo_6Se_8$-$EuMo_6Se_8$

J.-M. TARASCON, M. R. HARRISON, D. C. JOHNSON,* and M. J. SIENKO

Received July 18, 1983

Superconducting critical temperatures, measured by an ac mutual-inductance technique at ambient pressure, show for the series $La_{1-x}Eu_xMo_6Se_8$ approximately the same behavior as previously reported for the series $La_{1-x}Yb_xMo_6Se_8$; the decrease in the transition temperature with increasing x and the absence of superconductivity above 1.5 K for compositions with $x > 0.8$ may be explained solely in terms of the theory of Abrikosov and Gor'kov. This is not the case for the corresponding sulfide systems. None of the compositions in the series $Eu_{1.2}Mo_6(S_{1-x}Se_x)_8$ were found to be superconducting at ambient pressure above 1.5 K. Magnetic susceptibility measurements have been carried out by the Faraday method over the temperature range 2-300 K and confirm that the europium ions are divalent over the entire composition range for both series. X-Band electron spin resonance spectra obtained from the europium ions may be explained by assuming a spin Hamiltonian containing crystal field terms that are much larger than the Zeeman interaction term. In addition, measurements on the compositions in the series $Eu_{1.2}Mo_6(S_{1-x}Se_x)_8$ reveal the presence of a europium-containing impurity phase, $EuS_{1-x}Se_x$, in substantial quantities.

Introduction

A significant amount of theoretical and experimental effort has been expended over the past few years in an attempt to understand the absence of superconductivity in the europium Chevrel phases (see Figure 1), $Eu_yMo_6X_8$ ($1.0 < y < 1.2$; X = S, Se).[1] Since Eu^{2+} ions ($4f^7$, $^8S_{7/2}$) are isoelectronic with Gd^{3+} ions, magnetic considerations suggest that the superconducting critical temperatures T_c of the europium compounds should be similar to those observed in the corresponding gadolinium compounds ($Gd_{1.2}Mo_6S_8$, T_c = 1.4 K;[2] $Gd_{1.2}Mo_6Se_8$, T_c = 5.4 K[3]). Size and valence considerations suggest that T_c should be even higher.[4] Recently, several groups have applied pressure to the europium Chevrel phases and detected nonbulk superconductivity in the pure sulfide compound ($Eu_yMo_6Se_8$)[5-10] and in sulfide-rich mixed sulfide-selenide compounds.[11] However, no superconductivity has been detected to date in the pure selenide compound ($Eu_yMo_6Se_8$) at temperatures down to 1.2 K and at pressures up to 20 kbar.[12] The transition temperatures, critical pressures, and superconducting signal strength appear to depend sensitively upon the experimental technique, and it has been suggested[13] that the observed superconductivity might occur in the grain boundaries of the samples. Nevertheless, the superconductivity would seem to be associated with the Chevrel phase, since none of the impurity phases that are likely to be encountered in the materials exhibit similar superconducting properties.[13]

Several reasons have been advanced to explain the absence of superconductivity at ambient pressure and its onset at higher pressures in the pure sulfide and sulfide-rich mixed sulfide-selenide compounds. Initially it was believed that the lack of superconductivity was due to the magnetic nature of the europium ions; application of pressure might then change magnetically ordered Eu^{2+} ions into diamagnetic Eu^{3+} ions and thereby permit superconductivity. However, Mössbauer measurements showed no evidence of magnetic ordering down to 60 mK.[14] Furthermore, Chevrel phases containing diamagnetic alkaline-earth ions such as $BaMo_6X_8$ are also nonsuperconducting. Instead, Baillif et al.[15] attributed the absence of superconductivity in $Eu_yMo_6S_8$ and $BaMo_6S_8$ to a low-temperature structural-phase transition from rhombohedral to triclinic symmetry that opens a gap in the density of states at the Fermi level. Such a structural-phase transition might then be suppressed by the application of pressure, and indeed nonbulk superconductivity was subsequently observed in $BaMo_6S_8$ under pressure by Hor et al.[16]

In $Eu_yMo_6S_8$, the structural-phase transition could be correlated with a peak in the heat capacity observed at 108 K[17] and an abrupt *increase* in the electrical resistivity of the material below this temperature.[12,17] In contrast, the electrical resistivity of $Eu_yMo_6Se_8$ is observed to *decrease* rapidly below a similar temperature.[12] It is not known whether this is due to a similar structural-phase transition, but it does not appear that a gap opens in the density of states at the Fermi level in this material. Thus, another mechanism may be responsible for the absence of superconductivity in $Eu_yMo_6Se_8$.

In order to obtain more information about the unusual behavior of the europium Chevrel-phase compounds, we have undertaken an investigation of the magnetic properties of the mixed systems $Eu_{1.2}Mo_6(S_{1-x}Se_x)_8$ and $La_{1-x}Eu_xMo_6Se_8$. The results on the latter system can be compared to the results obtained on the $(La_{1-x}Eu_x)_{1.2}Mo_6S_8$ system[18-20] and on the

(1) See, for example: K. Yvon, *Curr. Top. Mater. Sci.*, **3**, 53 (1979); O. Fischer, *Appl. Phys.*, **16**, 1 (1978).
(2) O. Fischer, A. Treyvaud, R. Chevrel, and M. Sergent, *Solid State Commun.* **17**, 721 (1975).
(3) R. N. Shelton, R. W. McCallum, and H. Adrian, *Phys. Lett. A.*, **56A**, 213 (1976).
(4) J.-M. Tarascon, D. C. Johnson, and M. J. Sienko, *Inorg. Chem.*, **21**, 1505 (1982).
(5) C. W. Chu, S. Z. Huang, C. H. Lin, R. L. Meng, and M. K. Wu, *Phys. Rev. Lett.*, **46**, 276 (1981).
(6) D. W. Harrison, K. C. Lim, J. D. Thompson, C. Y. Huang, P. D. Hambourger, and H. L. Luo, *Phys. Rev. Lett.*, **46**, 280 (1981).
(7) M. S. Torikachvili and M. B. Maple, *Physica B+C (Amsterdam)*, **108B+C**, 1271 (1981).
(8) R. W. McCallum, W. A. Kalsbach, T. S. Radhakrishnan, F. Pobell, R. N. Shelton, and P. Klavins, *Solid State Commun.*, **42**, 819 (1982).
(9) M. K. Wu, P. H. Hor, R. L. Meng, T. H. Lin, V. Diatschenko, X. Y. Shao, X. C. Jin, and C. W. chu, *Phys. Rev. B: Condens. Matter*, **26**, 5230 (1982).
(10) R. C. Lacoe, S. A. Wolf, P. M. Chaikin, C. Y. Huang, and H. L. Luo, *Phys. Rev. Lett.*, **48**, 1212 (1982).
(11) R. L. Meng, T. H. Lin, M. K. Wu, C. W. Chu, and S. Z. Huang, *J. Low Temp. Phys.*, **48**, 383 (1982).
(12) C. W. Chu, S. Z. Huang, J. H. Lin, R. L. Meng, and M. K. Wu in "Ternary Superconductors", G. K. Shenoy, B. D. Dunlap, and F. Y. Fradin, Eds., North-Holland Publishing Co., Amsterdam, 1981, p 103.
(13) C. W. Chu, M. K. Wu, R. L. Meng, T. H. Lin, V. Diatschenko, and S. Z. Huang in "Physics of Solids under High Pressure", J. S. Schilling and R. N. Shelton, Eds., North-Holland Publishing Co., Amsterdam, 1982, p 357.
(14) R. W. McCallum, F. Claasen, and F. Pobell in "Ternary Superconductors", G. K. Shenoy, B. D. Dunlap, and F. Y. Fradin, Eds., North-Holland Publishing Co., Amsterdam, 1981, p 99.
(15) R. Baillif, A. Dunand, J. Muller, and K. Yvon, *Phys. Rev. Lett.*, **47**, 672 (1981).
(16) P. H. Hor, M. K. Wu, T. H. Lin, X. Y. Shao, X. C. Jin, and C. W. Chu, *Solid State Commun.*, **44**, 1605 (1982).
(17) R. Baillif, A. Junod, B. Lachal, J. Muller, and K. Yvon, *Solid State Commun.*, **40**, 603 (1981).
(18) M. S. Torikachvili and M. B. Maple, *Solid State Commun.*, **40**, 1 (1981).

0020-1669/84/1323-1094$01.50/0

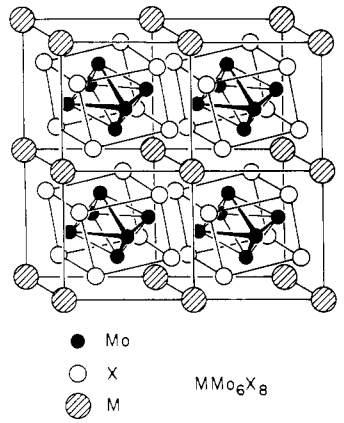

Figure 1. Chevrel-phase structure MMo_6X_8.

corresponding ytterbium systems where the Yb^{2+} ions are diamagnetic.[21]

Experimental Section

Sample Preparation. The compounds described here were prepared from ultrapure starting elements, as previously described.[4] Appropriate amounts of the elements to form 1-g samples of the mixed phases $Eu_{1.2}Mo_6(S_{1-x}Se_x)_8$ (x = 0, $^1/_8$, $^2/_8$, ...) and $La_{1-x}Eu_xMo_6Se_8$ (x = 0, 0.1, 0.2, ...) were placed in previously degassed silica tubes, and the tubes were degassed again at 10^{-6} torr and sealed. All the tubes for a given system were placed together in a box furnace, the temperature of which was slowly raised to 1050 °C over a period of 5 days. After 24 h at 1050 °C, the samples were quenched in air and the tubes vigorously shaken so as to homogenize the contents. They were immediately reheated to 1100 °C, kept there for 48 h, and then quenched in air. The samples were removed to a helium Dri-lab where they were opened and thoroughly ground. After being resealed in new degassed silica tubes, which were in turn sealed in bigger ones, the samples were heated as previously described. Finally, the samples were then heated at 1220 °C for 96 h and cooled in air. The resulting materials were fine, homogeneous gray-black powders.

Powder X-ray Diffraction. X-ray diffraction photographs were made by using a 114.6-mm diameter Debye-Scherrer camera with nickel-filtered Cu Kα radiation. Lines were indexed with the aid of a program that calculated the positions and intensities of possible reflections from available single-crystal data. A least-squares fit, with corrections for absorption and camera radius error, was performed by using all lines with $\theta(hkl) > 30°$ that could be indexed unambiguously.

Superconducting Transition Determination. The transition to the superconducting state was monitored by using an ac mutual-inductance apparatus, which has been described elsewhere.[22] In this device, the detection system is a primary coil with two opposed secondary coils wound symmetrically about it. The sample was placed in one of the secondary coils, and onset on superconductivity was signaled by an imbalance between the secondary coils due to an abrupt increase in the magnetic shielding that occurred when the sample became perfectly diamagnetic. Temperature was measured by using a calibrated CryoCal germanium thermometer, which was checked against the boiling point of helium and the transition temperature of lead and niobium. The T_c value was taken as the temperature at which the inductively measured transition was half-complete. The width of the transition was defined as the temperature difference between the points where the transition is 10% and 90% complete.

Magnetic Susceptibility. Magnetic susceptibilities were measured from 2 K (or T_c) to room temperature by the Faraday technique with use of the apparatus previously described.[23] Several major modifications, however, have been made in the instrument. The Cahn RG electrobalance has been replaced with a heavier capacity instrument donated to us by Bell Laboratories through the good office of Frank diSalvo. A new Janis Dewar has been installed with a Si sensor for measuring the temperatures, and a microprocessor has been installed to automate the data aquisition. Details of the reconstructed Faraday balance will be published elsewhere. The balance was calibrated by using $HgCo(SCN)_4$ as a standard. Samples were held in Spectrosil quartz buckets. All samples were run over a range of fields (5–10 kG); susceptibilities were found to be field independent. The reported susceptibilities have been corrected for the susceptibility of the quartz buckets.

Electron Spin Resonance. ESR spectra of powder samples sealed in Spectrosil silica tubes were recorded on a Varian E-12 spectrometer at X-band frequencies (9.3 GHz) using a 100-kHz modulation frequency. The temperature of the sample could be controlled to within 1 K over the range 10–300 K with the use of an Oxford Instruments ESR9 continuous-flow cryostat. The temperature was measured with a gold + 0.03% iron–chromel thermocouple positioned in the helium flow path just below the samples. The field was measured by a Varian NMR gaussmeter and the frequency by a Sistron Donner counter.

Results and Discussion

The X-ray data on the $Eu_{1.2}Mo_6(S_{1-x}Se_x)_8$ system indicate that the bulk samples were single phased over the whole range of composition $0 \leq x \leq 1$. This suggests that the amount of any impurity phase in the samples such as EuX or MoX_2 would be less than 5%. However, the X-ray detection of certain impurity phases in Chevrel-phase compounds MMo_6X_8 is made difficult by the large number of diffraction lines present in the patterns. In the case of the europium sulfide compounds, for example, the most intense diffraction lines for both EuS and MoS_2 all fall close to very strong $EuMo_6S_8$ diffraction lines. However, there are intense diffraction lines for Mo_2S_3 that are not obscured by the lines from $EuMo_6S_8$, and in order to eliminate the easily observed Mo_2S_3 impurity phase, researchers have added an excess of europium metal. This practice is particularly common in the case of all the rare-earth compounds, where the reaction is comparatively slow. Neutron diffraction data for several rare-earth sulfide and selenide compounds all indicate that the actual stoichiometry is $RE_{1.0}Mo_6X_8$.[24] In addition, a rare-earth impurity phase was observed in the samples that was not observed in the X-ray diffraction patterns. The following equilibrium probably occurs in the reaction to form the Chevrel phases:

$$1.2M + 6Mo + 8X = 1.2MX + MoX_2 + Mo_2X_3 + Mo = M_{1.0}Mo_6X_8 + MX + Mo \quad (1)$$

The amount of the impurity phases MX and Mo is less than 5% of the total sample and therefore difficult to detect by X-rays, but the phase MX contains about 20% of the rare-earth element. For the mixed europium sulfide–selenide samples studied here, the presence of $EuS_{1-x}Se_x$ is indicated by both magnetic susceptibility and ESR measurements.

The unit cell parameters for the series $Eu_{1.2}Mo_6(S_{1-x}Se_x)_8$ are shown in Figure 2. The patterns could be indexed completely on the basis of either a hexagonal or rhombohedral unit cell with no detectable impurity lines. The unit cell volume is linearly dependent on the composition parameter x, suggesting that the oxidation state of europium remains constant across the series. However, when about half of the sulfur atoms have been replaced by selenium, the rhombohedral angle (α_r) passes through a maximum and the hexagonal parameter (c/a) passes through a minimum. These results are quite similar to those observed for ytterbium,[4] which is also divalent; they are unlike those found for lanthanum[25] where preferential

(19) M. S. Torikachvili, M. B. Maple, R. P. Guertin, and S. Foner, *J. Appl. Phys.*, **53**, 2619 (1982).
(20) M. S. Torikachvili, M. B. Maple, R. P. Guertin, and S. Foner, *J. Low Temp. Phys.*, **49**, 573 (1982).
(21) J.-M. Tarascon, D. C. Johnson, and M. J. Sienko, *Inorg. Chem.*, **22**, 3769 (1983).
(22) W. G. Fisher, Ph.D. Thesis, Cornell University, 1978.
(23) J. E. Young, Ph.D. Thesis, Cornell University, 1971.
(24) See, for example: J. D. Jorgensen, D. G. Hinks, D. R. Noakes, P. J. Viccaro, and G. K. Shenoy, *Phys. Rev. B: Condens. Matter*, **27**, 1465 (1983); J. W. Lynn, G. Shirane, W. Thomlinson, R. N. Shelton, and D. E. Moncton, *ibid.*, **24**, 3817 (1981).
(25) D. C. Johnson, J. M. Tarascon, and M. J. Sienko, *Inorg. Chem.*, **22**, 3773 (1983).

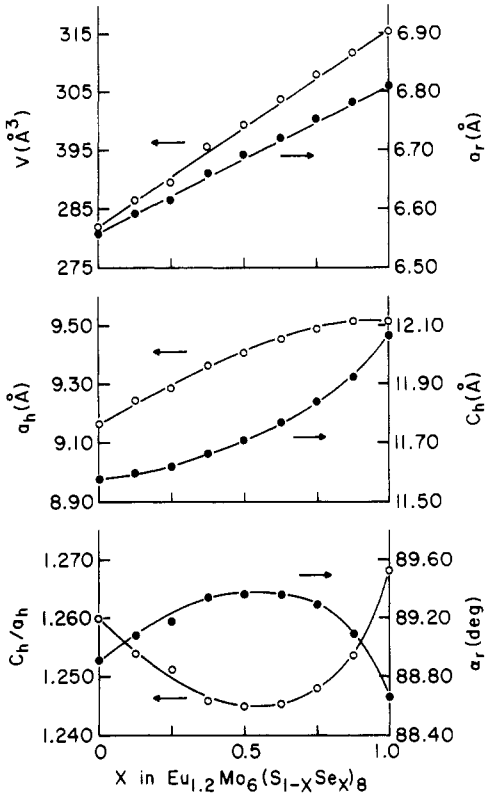

Figure 2. Unit cell parameters as a function of x in $Eu_{1.2}Mo_6(S_{1-x}Se_x)_8$. The size of the data points exceeds the error in the fitted values.

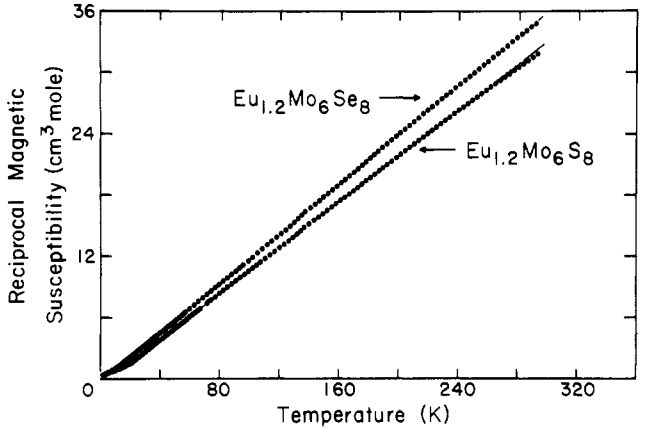

Figure 3. Reciprocal molar magnetic susceptibility for samples of $Eu_{1.2}Mo_6S_8$ and $Eu_{1.2}Mo_6Se_8$ as a function of temperature.

ordering of the sulfur in the special chalcogen position (see Figure 9) produces breaks in the curves of these two parameters plotted as a function of the composition parameter x. Thus, crystallographically, europium ions in the Chevrel phases behave as divalent rather than trivalent ions. This is confirmed by the magnetic susceptibility and ESR measurements.

Magnetic susceptibility measurements were made over the temperature range 2–300 K on five samples, with $x = 0.0$, 0.25, 0.5, 0.75, and 1.0. Some of the results are shown in Figure 3. The measured molar magnetic susceptibility has been corrected for the diamagnetism of the ion cores[26] and then the reciprocal of the susceptibility has been plotted as a function of temperature. Above 40 K, the data points may be fitted to a single straight line, indicating that the data accurately obey the Curie law, $\chi = C/T$ in this temperature range. An effective magnetic moment may then be calculated as

(26) P. W. Selwood in "Magnetochemistry", Interscience, New York, 1956, p 78.

Table I. Magnetic Susceptibility Data for Samples of $Eu_{1.2}Mo_6(S_{1-x}Se_x)_8$

x	C, cm³ mol⁻¹	μ_B	x	C, cm³ mol⁻¹	μ_B
0.0	9.105	7.79	0.75	8.328	7.45
0.25	9.012	7.75	1.0	8.330	7.45
0.5	9.388	7.91			

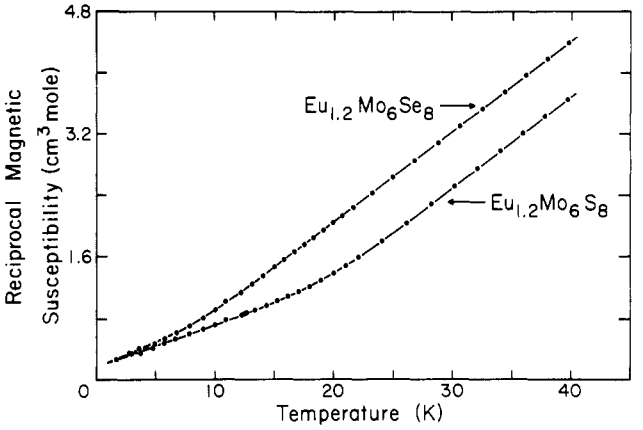

Figure 4. Reciprocal molar magnetic susceptibility for samples of $Eu_{1.2}Mo_6S_8$ and $Eu_{1.2}Mo_6Se_8$ as a function of temperature below 40 K.

$2.828C^{1/2}$, after correcting the measured value of C for the number of moles of europium in the samples. Table I summarizes the magnetic parameters derived from all of the samples of $Eu_{1.2}Mo_6(S_{1-x}Se_x)_8$ studied in this investigation. The observed values for the magnetic moments are somewhat less than the theoretical value of 7.94 μ_B expected for the ground term of Eu^{2+} ($4f^7$, $^8S_{7/2}$). However, the value obtained for the moment of $Eu_{1.2}Mo_6Se_8$ is in good agreement with that previously reported by Johnston and Shelton.[27] They explained the reduction of the observed moment by postulating the presence of 12% Eu^{3+} ions in their sample. Eu^{3+} ions in their ground state ($4f^6$, $^7S_0$) are nonmagnetic because of the mutual cancellation of the orbital and spin moments. This might arise from the presence in the sample of a small quantity of Eu_2O_2S, which contains Eu^{3+} ions. McCallum et al.[8] analyzed the composition of several nonstoichiometric europium sulfide compounds and detected several impurity phases: Mo, Mo_2S_3, MoS_2, and Eu_2O_2S. A second possible reason for the reduction of the observed moment is the loss of a small quantity of europium as a film of EuX found on the walls of the quartz reaction tubes. The required weight loss of EuX to explain the reduction of the observed moments amounts to less than 0.01 g of EuX from the 1 g samples. If the reduction of the moment in Johnston and Shelton's sample is due to the loss of 12% of the europium from their original stoichiometry, the final stoichiometry of the sample would be $Eu_{1.06}Mo_6Se_8$, much closer to the stoichiometry of $M_{1.0}Mo_6Se_8$ observed by neutron diffraction for the rare-earth Chevrel phases.[24]

Figure 4 shows the susceptibility data below 40 K. The kinks in the curves are due to the presence of an EuX impurity phase. The most pronounced kink occurs in $Eu_{1.2}Mo_6S_8$ at 18 K; this is good evidence for the presence of EuS, which is known to order ferromagnetically at 16.5 K.[28,29] Moreover, the ESR results are compatible with this hypothesis. Figure 5 shows the first-derivative X-band ESR spectra of five samples of $Eu_{1.2}Mo_6(S_{1-x}Se_x)_8$ at 40 K. The spectra are qualitatively similar and may be separated into two components:

(27) D. C. Johnston and R. N. Shelton, *J. Low Temp. Phys.*, **26**, 561 (1977).
(28) K. Kojima, T. Hihara, and T. Kamigaichi, *J. Phys. Soc. Jpn.*, **49**, 2419 (1980).
(29) H. Fujiwara, H. Kadomatsu, M. Kurishu, T. Hihara, K. Kojima, and T. Kamigaichi, *Solid State Commun.*, **42**, 509 (1982).

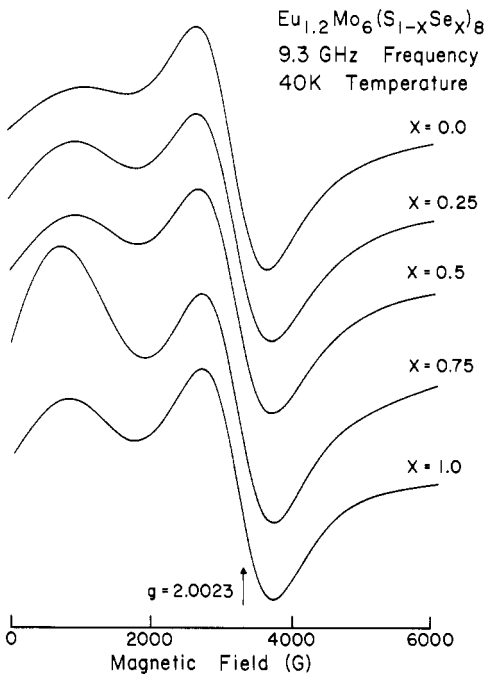

Figure 5. ESR spectra of samples of $Eu_{1.2}Mo_6(S_{1-x}Se_x)_8$ at 40 K.

a resonance arising from the Chevrel phase and a resonance arising from the same impurity phase identified in the magnetic susceptibility measurements on these samples. The Chevrel-phase resonance is anisotropic and spread over the entire scan range from 0 to 6000 G; part of the resonance appears as the peak in the spectra at approximately 1000 G. This resonance will be considered in more detail later in this paper. The impurity-phase resonance is isotropic and is centered at approximately 3200 G; the isotropic g value of the resonance is therefore close to the free-spin value of $g = 2.0023$.

We identify the impurity phase as $EuS_{1-x}Se_x$. Kojima et al.[28,29] have studied the magnetic properties of this system and have shown that the sulfide-rich compositions are ferromagnetic while the selenide-rich compositions are antiferromagnetic. EuS has a Curie temperature of 16.5 K, and EuSe has a Néel temperature of 4.6 K. In $Eu_{1.2}Mo_6S_8$ and $Eu_{1.2}Mo_6(S_{0.75}Se_{0.25})_8$, the impurity-phase resonance shifts to a lower magnetic field below 20 K; the internal magnetic field produced by the ferromagnetic alignment of the Eu^{2+} ions adds to the external magnetic field produced by the spectrometer magnet and causes the resonance to occur at a lower external magnetic field than expected. In the remaining compositions, the impurity-phase resonance showed no shift at the lowest accessible temperature of the cryostat, viz. 10 K.

The amount of the impurity phase in the samples is difficult to estimate from the ESR spectra, since the Chevrel-phase resonance is spread over a much larger magnetic field range than the impurity-phase resonance and hence appears much weaker. Nevertheless, a substantial quantity of the impurity phase is present in the samples as would be anticipated if the actual stoichiometry of the Chevrel phase were $EuMo_6X_8$ rather than $Eu_{1.2}Mo_6X_8$.

In order to cast more light on this problem of stoichiometry and also to investigate the effect of the Eu^{2+} magnetic moment on the superconducting properties of the Chevrel phases, we have undertaken an investigation of the $La_{1-x}Eu_xMo_6Se_8$ system. The results can be compared with those obtained on $La_{1-x}Yb_xMo_6Se_8$;[21] in this sytem the Yb^{2+} ions are diamagnetic.

The X-ray data on the $La_{1-x}Eu_xMo_6Se_8$ system indicate that the bulk samples were all single phased over the whole range of composition $0 \leq x \leq 1$. The unit cell parameters for the series are shown in Figure 6; the patterns could again be

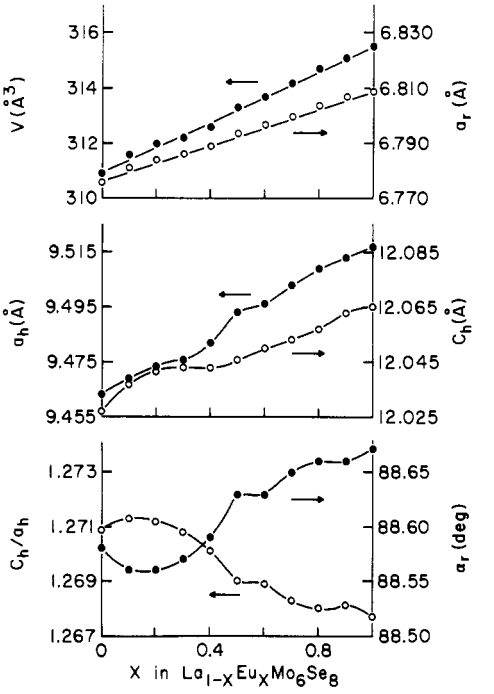

Figure 6. Unit cell parameters as a function of x in $La_{1-x}Eu_xMo_6Se_8$. The size of the data points exceeds the error in the fitted values.

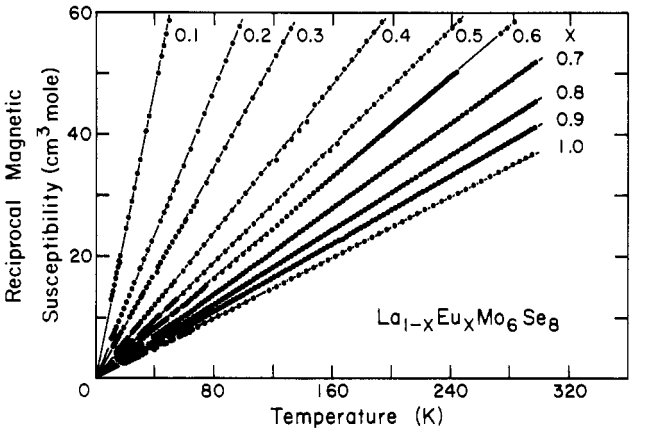

Figure 7. Reciprocal molar magnetic susceptibility for samples of $La_{1-x}Eu_xMo_6Se_8$ as a function of temperature.

indexed completely on the basis of either a hexagonal or rhombohedral cell with no detectable impurity lines. The magnetic susceptibility data for some of these samples are shown in Figure 7. For samples in the composition range $1 \geq x \geq 0.2$, the susceptibility was fitted to a Curie law over the entire temperature range of the data from 2 to 300 K. Unlike the $Eu_{1.2}Mo_6(S_{1-x}Se_x)_8$ series discussed earlier, there is no evidence in the low-temperature data for the presence of an EuSe impurity phase. This conclusion is also supported by the ESR measurements on these samples described below. For the samples with $x = 0.1$ and 0.0, additional terms were required to allow for the temperature-independent paramagnetism of the samples. Strictly, these terms are required for all of the metallic samples with $x < 1$, but the Curie-law contribution from the europium ions in the samples was so large that the fitted values obtained for these terms were not reliable. The magnetic parameters for the $La_{1-x}Eu_xMo_6Se_8$ series are summarized in Table II. Within compositional error, the observed moments are all in good agreement with the theoretical moment of 7.94 μ_B for Eu^{2+} ions.

Figure 8 shows the first-derivative X-band ESR spectra of five samples of $La_{1-x}Eu_xMo_6Se_8$. The spectra are again qualitatively similar, with the line width of the resonance

Table II. Magnetic Susceptibility Data for Samples of $La_{1-x}Eu_xMo_6Se_8$

x	C, cm^3 mol^{-1}	magn moment, μ_B	x	C, cm^3 mol^{-1}	magn moment, μ_B
0.0	9.718×10^{-3}		0.6	4.624	7.9
			0.7	5.714	8.1
0.1	0.820	8.1	0.8	6.531	8.1
0.2	1.682	8.2	0.9	7.202	8.0
0.3	2.306	7.8	1.0	7.982	8.0
0.4	3.306	8.1			
0.5	4.183	8.2			

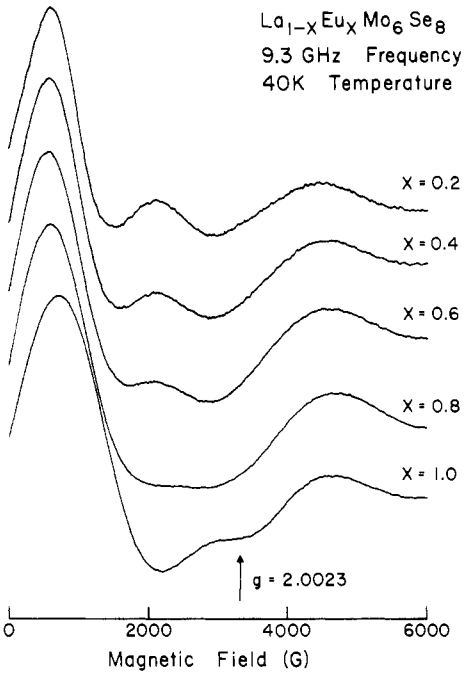

Figure 8. ESR spectra of samples of $La_{1-x}Eu_xMo_6Se_8$ at 40 K.

monotonically increasing with x as the concentration of europium ions in the samples increases. However, the spectra are considerably different from the spectra of the samples of $Eu_{1.2}Mo_6(S_{1-x}Se_x)_8$ (Figure 5); the change in the stoichiometry of the samples from $M_{1.2}Mo_6X_8$ to $M_{1.0}Mo_6X_8$ has resulted in the disappearance of the $EuS_{1-x}Se_x$ impurity phase.

The most striking aspect of these spectra is the pronounced anisotropy exhibited by the resonance. Normally, the resonance from the rare-earth ions with a $4f^7$ electronic configuration is centered at $g = 2$ since the splitting of the energy levels caused by the Zeeman interaction is much larger than the splitting of the energy levels caused by the crystal field.[30] However, we will show that the X-band spectra of the europium Chevrel phases may be interpreted by considering a spin Hamiltonian that has crystal field terms much larger in magnitude than the Zeeman interaction term.

The crystal field at the europium sites in the Chevrel phases is produced by a trigonally distorted cube of chalcogen ions as shown in Figure 9. Two of the chalcogen ions occupy special positions on the trigonal axis; the remaining six occupy general positions. If the trigonal distortion is sufficiently large, we may drop all of the terms in the spin Hamiltonian that are higher than second order in the spin operators. The spin Hamiltonian then becomes

$$\mathcal{H} = g_0\mu_B BS + D(S_z^2 - \tfrac{1}{3}S(S+1)) + E(S_x^2 - S_y^2) \quad (2)$$

The term in E is included to allow for a reduction in the

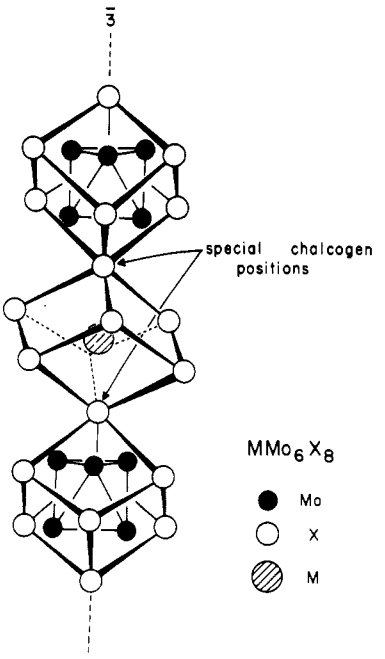

Figure 9. Part of the Chevrel-phase structure MMo_6X_8, showing the axially distorted cube of chalcogen ions surrounding the M ions and distinguishing the special chalcogen positions on the axis from the general chalcogen positions.

symmetry of the crystal field from trigonal to rhombic. It is conventional to define a dimensionless parameter $\lambda = E/D$; for pure trigonal symmetry $\lambda = 0$, and for pure rhombic symmetry $\lambda = 1/3$. Wickman et al.[31] have demonstrated that this range for λ covers all of the physically distinct possibilities. Further simplification of the spin Hamiltonian is possible in two cases:

(1) Weak Crystal Field Case: $g_0\mu_B B >> D,E$. The Zeeman interaction lifts the degeneracy of the $S = 7/2$ ground state of the Eu^{2+} ions, producing eight levels labeled by their value of M_S ($|-7/2\rangle$, $|-5/2\rangle$, $|-3/2\rangle$, $|-1/2\rangle$, $|1/2\rangle$, $|3/2\rangle$, $|5/2\rangle$, $|7/2\rangle$) and uniformly separated by $h\nu = g_0\mu_B B$. The crystal field may then be applied as a perturbation; the result is resonance approximately centered at $g = 2$ that exhibits some fine structure splitting.

(2) Strong Crystal Field Case: $g_0\mu_B B << D,E$. The crystal field lifts the degeneracy of the ground state, producing four doublets ($|\pm 1/2\rangle$, $|\pm 3/2\rangle$, $|\pm 5/2\rangle$, $|\pm 7/2\rangle$) separated by different energies. The $|\pm 1/2\rangle$ and $|\pm 3/2\rangle$ doublets are separated by $2D$ if $\lambda = 0$. The Zeeman interaction may then be applied as a perturbation. If the crystal field splitting is large compared to the energy of the microwave quantum $h\nu = g_0\mu_B B$, no transitions occur between the different doublets. Each doublet then behaves as an isolated system with $S = 1/2$ and an anisotropic effective g value; the result is a resonance that is spread over a large magnetic field range and contains a contribution from each of the four doublets. This case is encountered in the europium Chevrel phases.

Nicklin et al.[32] have considered the strong crystal field case in connection with the resonances observed from Gd^{3+} ions in glasses. We have repeated the calculations outlined in their paper, and in Figure 10 we show the principal g values obtained for the $|\pm 1/2\rangle$ and $|\pm 3/2\rangle$ doublets for values of λ between 0 and 0.1. The transition probability for a resonance within each doublet is essentially determined by the degree

(30) A. Abragam and B. Bleaney in "Electron Paramagnetic Resonance of Transition Ions", Clarendon Press, Oxford, 1970, p 335.

(31) H. H. Wickman, M. P. Klein, and D. A. Shirley, *J. Chem. Phys.* **42**, 2113 (1965).

(32) R. C. Nicklin, J. K. Johnstone, R. G. Barnes, and D. R. Wilder, *J. Chem. Phys.*, **59**, 1652 (1973).

(33) R. Odermatt, *Helv. Phys. Acta*, **54**, 1 (1981).

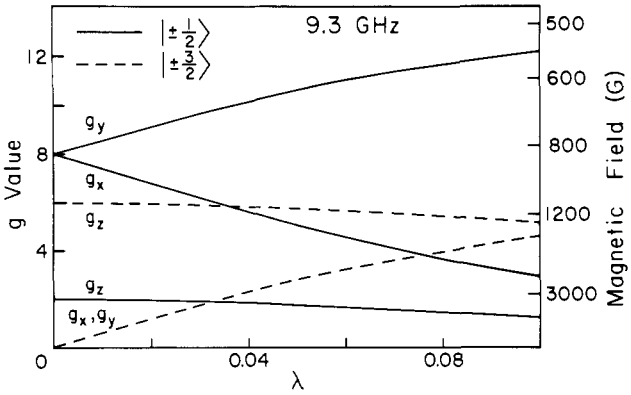

Figure 10. Calculated g values for the $|\pm^1/_2\rangle$ and $|\pm^3/_2\rangle$ doublets as a function of λ.

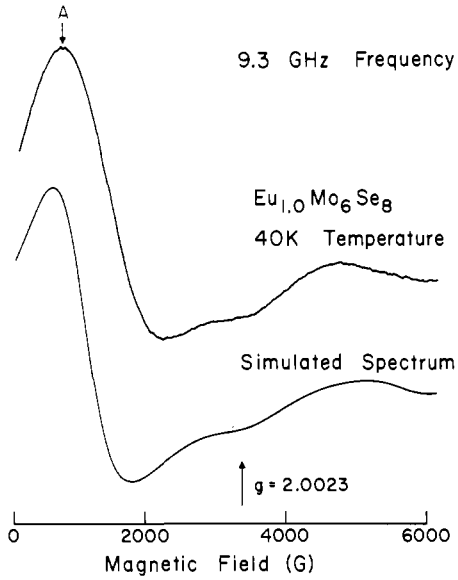

Figure 11. Observed ESR spectrum of $EuMo_6Se_8$ at 40 K, compared with a calculated ESR spectrum (see text).

of mixing of the pure states (M_S = $^1/_2$, $^3/_2$, $^5/_2$, ...) between the doublets. If λ = 0, no mixing of the pure states occurs so transitions are allowed only within the $|\pm^1/_2\rangle$ doublet by virtue of the rule $\Delta M_S = 1$. If λ ≠ 0, mixing occurs and transitions within the remaining doublets are possible. However, for the values of λ encountered in the europium Chevrel phases, only transitions within the $|\pm^1/_2\rangle$ and $|\pm^3/_2\rangle$ doublets occur with any significant probability.

In Figure 11, we have calculated a spectrum using this model and compared it to the experimental spectrum obtained from $EuMo_6Se_8$ at 40 K. The parameters of the model that were used in the simulation were λ = 0.02 and an isotropic line width ($\Delta B_{1/2}$) of 750 G with a Lorentzian line shape. The calculated spectrum is dominated by the contribution from the $|\pm^1/_2\rangle$ doublet; however, it was found necessary to add a small (5%) contribution from the $|\pm^3/_2\rangle$ doublet in order to reproduce the downturn in the experimental spectrum at 5500 G. Allowing for the simplified nature of the model, the agreement with the experimental spectrum is satisfactory. A more complete model would have to consider the crystal field and Zeeman interaction terms on an equal footing, consider higher order terms in the spin operators in the spin Hamiltonian, and use a Dysonian line shape rather than a Lorentzian line shape for the metallic samples with $x < 1$.

Changes occur in the spectra as a function of both composition and temperature. An easily measurable feature of the Chevrel-phase resonance, even when the $EuS_{1-x}Se_x$ impurity phase is present in the samples, is the position of the

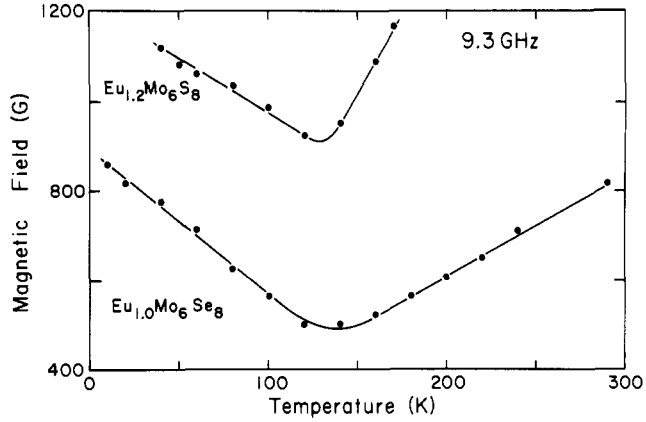

Figure 12. Position of the low-field peak in the ESR spectra of $EuMo_6Se_8$ and $Eu_{1.2}Mo_6S_8$ as a function of temperature.

peak at low magnetic fields (labeled A in Figure 11). This feature was invariably found to occur between 600 and 1400 G, which is compatible with the range of g values predicted by the model (see Figure 10); small changes in the values of λ produce large changes in the position of the peak. Typical results for $Eu_{1.2}Mo_6S_8$ and $EuMo_6Se_8$ are shown in Figure 12. The position of the peak in both samples has a minimum near 120 K, and it is interesting that resistance anomalies occur in both samples near this temperature.[12]

The validity of this model essentially depends upon the fact that the magnitude of the microwave quantum is insufficient to allow transitions between the doublets. Thus, ESR measurements at a higher microwave frequency are likely to produce a very different spectrum. There have been two previous ESR studies on the Chevrel phases. Odermatt et al.[34-36] studied the Q-band (35 GHz) and V-band (60 GHz) spectra of Eu^{2+} and Ga^{3+} ions as dopants in the lead and tin Chevrel-phase sulfides. They observed a resonance centered approximately at $g = 2$ that exhibited pronounced fine structure. Using the same spin Hamiltonian (eq 2) in the weak crystal field case, they were able to fit the Eu^{2+} spectra for both the lead and tin Chevrel phases with $D = 0.10$ cm^{-1} and λ ≤ 0.05. They were similarly able to fit the Gd^{3+} spectra with $D = 0.07$ cm^{-1} and λ ≤ 0.05. Thus, the crystal field splitting is stronger for Eu^{2+} ions than Gd^{3+} ions. Since the microwave quanta have energies of 0.3 and 1.2 cm^{-1} for X band and Q band, respectively, the microwave quantum is similar in magnitude to the crystal field splitting ($2D$) for X band but greater than the crystal field splitting for Q band.

Ozeroff et al.[35] studied the X-band and Q-band spectra of $Gd_{1.2}Mo_6Se_8$ and $Gd_{1.0}Mo_6Se_8$ and observed a resonance centered at $g = 2$ with no visible fine structure splitting. The line shape was Dysonian, and the line width increased linearly with temperature according to the relation $\Delta B_{1/2} = a + bT$, which is characteristic of an exchange interaction between the Gd^{3+} ions and the conduction electrons.[36] From the measured value of b (1.9GK^{-1}), they were able to extract a value for the exchange integral of 0.011 eV, very similar to the value of 0.010 eV deduced from the depression of the superconducting critical temperature (T_c) according to the Abrikosov–Gor'kov theory.[37] It is much more difficult to attempt a similar analysis for the metallic samples of $La_{1-x}Eu_xMo_6Se_8$ because of the anisotropic nature of the resonance. However, the value of b for $La_{0.8}Eu_{0.2}Mo_6Se_8$ was estimated to be approximately

(34) R. Odermatt, M. Hardimann, and J. van Meijel, *Solid State Commun.*, **32**, 1227 (1979).
(35) S. Ozeroff, R. Calvo, D. C. Johnston, M. B. Maple, R. W. McCallum, and R. N. Shelton, *Solid State Commun.*, **27**, 201 (1978).
(36) S. E. Barnes, *Adv. Phys.*, **30**, 801 (1981).
(37) A. A. Abrikosov and L. P. Gor'kov, *Zh. Eksp. Teor. Fiz.*, **39**, 1781 (1960); *Sov. Phys.—JETP (Engl. Transl.)*, **12**, 1243 (1961).

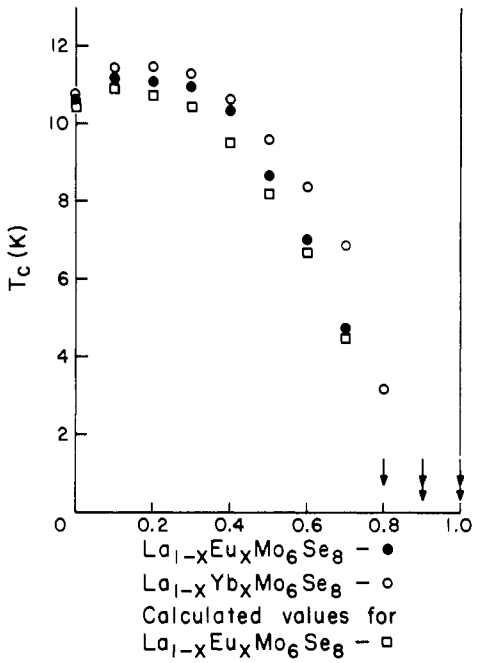

Figure 13. Superconducting critical temperatures as a function of x in $La_{1-x}Eu_xMo_6Se_8$ and $La_{1-x}Yb_xMo_6Se_8$,[21] compared with the calculated values (see text).

twice that for $Gd_yMo_6Se_8$; the exchange integral is therefore estimated to slightly larger in $La_{0.8}Eu_{0.2}Mo_6Se_8$ than in $Gd_yMo_6Se_8$.

The most interesting results for this series concern the variation with composition of the superconducting transition temperatures, which are presented in Figure 13. The T_c values for $La_{1-x}Eu_xMo_6Se_8$ samples initially rise slightly (for $x = 0.1$ and 0.2), fall slightly (for $x = 0.3$ and 0.4), and then drop very rapidly with increasing x. The curve is quite similar to that observed for $La_{1-x}Yb_xMo_6Se_8$, except that the T_c values, particularly for $x \geq 0.5$, are higher. This difference in the T_c values between the europium and ytterbium systems can be explained in terms of the theory of Abrikosov and Gor'kov;[37] the depression is attributed to the exchange interaction between the rare-earth ion (Eu^{2+}) and the conduction electrons. The depression in T_c is given by the relation

$$\Delta T_c = n(N(E_F))I_2(g - 1)^2J(J + 1) \qquad (3)$$

where n is the concentration of rare-earth ions, $N(E_F)$ is the density of states at the Fermi level, I is the exchange integral, and $(g - 1)^2J(J + 1)$ is the de Gennes factor. A systematic application of this theory to the Chevrel phases by Maple et al.[38] indicates that the variation of ΔT_c with rare-earth ion can

(38) M. B. Maple, L. E. Delong, W. A. Fertig, D. C. Johnston, R. W. McCallum, and R. N. Shelton in "Valence Instabilities and Related Narrow Band Phenomena", R. D. Parks, Ed., Plenum Press, New York, 1977, p 17.

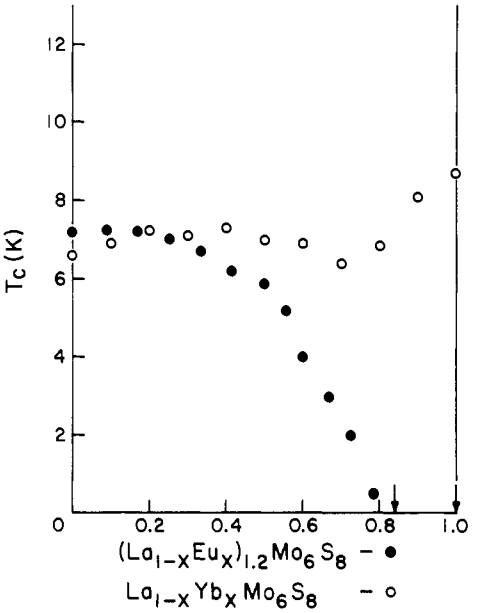

Figure 14. Superconducting critical temperatures as a function of x in $(La_{1-x}Eu_x)_{1.2}Mo_6S_8$[20] and $La_{1-x}Yb_xMo_6S_8$.[21]

be described qualitatively by the de Gennes factor; T_c is 3 K in the case of Gd^{3+}. In our case, the expected values of T_c are shown by the squares in Figure 13; we have calculated these values assuming $\Delta T_c = 0$ for the $La_{1-x}Yb_xMo_6Se_8$ series, where $J = 0$ for Yb^{2+}. The agreement between the observed values of T_c for $La_{1-x}Eu_xMo_6Se_8$ and the values predicted by the Abrikosov–Gor'kov theory, especially for high x, indicates that the pair-breaking interaction of eq 3 is sufficient to explain the absence of superconductivity in $EuMo_6Se_8$.

A different conclusion obtains for the corresponding sulfide series. The T_c values for $(La_{1-x}Eu_x)_{1.2}Mo_6S_8$ samples[21] are shown in Figure 14, together with the T_c values for $La_{1-x}Yb_xMo_6S_8$ samples.[22] Since the magnitude of the T_c depression calculated by using the theory of Abrikosov and Gor'kov is the same for corresponding compositions in both the sulfide and selenide systems, it is apparent that the absence of superconductivity in $EuMo_6S_8$ cannot be explained solely by the pair-breaking interaction of eq 3; as previously indicated in this paper, a crystal distortion occurs at 108 K that may be suppressed by the application of pressure. Whether or not a similar crystal distortion occurs in $EuMo_6Se_8$, the pair-breaking interaction would appear to be sufficient to suppress superconductivity. Therefore, it is unlikely that superconductivity can be induced in this material by the application of pressure, as is found to be the case experimentally.

Acknowledgment. This research was sponsored by the Air Force Office of Scientific Research, Grant No. AFOSR 80-0009, and was supported in part by the National Science Foundation and the Materials Science Center at Cornell University.